Plant Biotechnology 34, 89–95 (2017)
DOI: 10.5511/plantbiotechnology.17.0501a

Original Paper

Constitutive activation of plant-specific RAB5 GTPase confers increased resistance against adapted powdery mildew fungus

Noriko Inada[1]*, Kazuo Ebine[2,3], Emi Ito[4], Akihiko Nakano[5,6], Takashi Ueda[2,3,7]**

[1]The Graduate School of Biological Sciences, Nara Institute of Science and Technology, Nara 630-0192, Japan; [2]Division of Cellular Dynamics, National Institute for Basic Biology, Aichi 444-8585, Japan; [3]Department of Basic Biology, SOKENDAI (Graduate University for Advanced Studies), Aichi 444-8585, Japan; [4]Department of Natural Sciences, International Christian University, Tokyo 181-8585, Japan; [5]Department of Biological Sciences, Graduate School of Science, The University of Tokyo, Tokyo 113-0033, Japan; [6]Live Cell Super-Resolution Imaging Research Team, RIKEN Center for Advanced Photonics, Saitama 351-0198, Japan; [7]Japan Science and Technology Agency (JST), PRESTO, Saitama 332-0012, Japan
*E-mail: norikoi@bs.naist.jp Tel: +81-743-72-5592 Fax: +81-743-72-5599
**E-mail: tueda@nibb.ac.jp Tel: +81-564-55-7530 Fax: +81-564-55-7531

Received April 3, 2017; accepted May 1, 2017 (Edited by K. Hiratsuka)

Abstract The obligate biotrophic fungal pathogens that cause powdery mildew disease establish infection in living host cells by modifying host cellular functions, including membrane trafficking. Previously, we reported that two *Arabidopsis thaliana* RAB5 GTPases, plant-specific ARA6/RABF1 and canonical ARA7/RABF2b, accumulate at the extrahaustorial membrane (EHM), which surrounds the specialized infection hypha called the haustorium. In this study, we examined the role of ARA6 and ARA7, which regulate distinctive endosomal trafficking pathways, in plant–powdery mildew fungus interactions. Although ARA6- and ARA7-related mutants did not exhibit altered susceptibility to the *A. thaliana*–adapted powdery mildew fungus *Golovinomyces orontii*, overexpression of constitutively active ARA6, but not constitutively active ARA7, repressed proliferation of *G. orontii*. The repression of fungal proliferation was associated with accelerated formation of the callosic encasement around the haustorium. Furthermore, microscopic observation revealed an accumulation of the constitutively active form of ARA6, but not active ARA7, at the EHM. These results indicate that plant-specific ARA6 has a specific role in plant–powdery mildew fungus interaction, and manipulation of ARA6 activity could be a novel tool to overcome this plant disease.

Key words: *Arabidopsis thaliana*, extrahaustorial membrane, *Golovinomyces orontii*, powdery mildew, RAB5.

Introduction

Powdery mildew is a disease caused by ascomycete fungi of the order Erysiphales, and it produces distinctive white powdery structures on leaves, stems, and fruits. Powdery mildew fungi infect nearly 10,000 angiosperm plants including crops, vegetables, fruits, and ornamental plants, and they cause significant harvest loss and are thus very important pathogens (Takamatsu 2004).

To combat the powdery mildew disease, understanding the plant response mechanism to the fungal infection is critical, and numerous plant factors that function in either susceptibility or resistance to powdery mildew disease have been isolated and analyzed. *Mildew resistance locus o* (*Mlo*) is a well-known example, whose mutation causes increased resistance against powdery mildew fungi in various plants, including barley, tomato, pea, and the model experimental plant *Arabidopsis thaliana* (Acevedo-Garcia et al. 2014). Another factor that is involved in resistance against a wide variety of powdery mildew fungi is RESISTANCE TO POWDERY MILDEW8.2 (RPW8.2). The expression of *RPW8.2* confers resistance to multiple *A. thaliana*–adapted powdery mildew fungi (Xiao et al. 2001). However, utilization of these factors for improving plant resistance is not easy: loss of *Mlo* expression results in multiple phenotypes including early senescence, and ectopic expression of *RPW8.2* causes sporadic cell death. Therefore, a search for novel host factors involved in powdery mildew resistance is necessary.

Obligate biotrophic powdery mildew fungi establish parasitic relationships with living host plant cells

Abbreviations: dpi, days post inoculation; EHM, extrahaustorial membrane; GEF, guanine nucleotide exchange factor; GFP, green fluorescent protein; PI, propidium iodide; SA, salicylic acid; SNARE, soluble *N*-ethylmaleimide-sensitive factor attachment protein receptor; wpi, weeks post inoculation.
This article can be found at http://www.jspcmb.jp/
Published online June 28, 2017

through the formation of haustoria, which are thought to be responsible for delivery of effector proteins into and uptake of nutrients from host cells (Yi and Valent 2013). The function of a haustorium is fulfilled through the host-derived membrane that surrounds it, the extrahaustorial membrane (EHM). Recently, we reported that two plant RAB5 GTPases, the plant-specific ARA6/RABF1 (At3g54840) and the canonical ARA7/RABF2b (At4g19640), localize to the EHM formed by the *Arabidopsis thaliana*–adapted powdery mildew fungus *Golovinomyces orontii*. These molecules were present on the EHM throughout the formation and maturation of the haustorium, but were excluded from the EHM once the haustorium became surrounded by the callosic encasement, which is thought to be formed as a result of plant immunity (Meyer et al. 2009), indicating a positive correlation between RAB5 accumulation at the EHM and the functionality of the haustorium. In addition, plant-specific ARA6 localized to the EHM formed by barley-adapted *Blumeria graminis* f. sp. *hordei* and the obligate biotrophic oomycete *Hyaloperonospora arabidopsidis* in *A. thaliana* (Inada et al. 2016a). These results suggest a conserved function for ARA6 in interactions between plants and these biotrophic pathogens.

RAB5 is a key regulator of a wide range of endocytic events in eukaryotic organisms including plants (Ebine and Ueda 2009). In addition to canonical RAB5, which is highly conserved among eukaryotic lineages, plants have acquired a plant-specific RAB5 with a unique fatty-acylated N-terminal extension that is responsible for the membrane anchoring of this protein (Ueda et al., 2001). The *A. thaliana* genome contains three RAB5 GTPases: canonical ARA7 and RHA1/RABF2a (At5g45130), and plant-specific ARA6. Canonical RAB5s and plant-specific ARA6 localize to different but overlapping populations of multivesicular endosomes (Ebine et al. 2011; Haas et al. 2007; Ueda et al. 2004). In accordance with their distinct localizations, the two types of plant RAB5s regulate distinct trafficking events: RHA1 and ARA7 act in endocytic/vacuolar trafficking pathways (Ebine et al. 2011; Kotzer et al. 2004; Sohn et al. 2003), whereas ARA6 is involved in the trafficking pathway from the endosomes to the plasma membrane (Ebine et al. 2011). ARA6 may also play a role in vacuolar trafficking (Bottanelli et al. 2011).

Our previous finding showed both plant-specific ARA6 and canonical ARA7 localize to the EHM. However, the functions of these RAB5s on the EHM remain to be examined. In the present study, we investigated the susceptibility of various RAB5-related mutants and transgenic plants to *G. orontii* in order to elucidate the role of RAB5-mediated trafficking in plant–powdery mildew fungus interactions. We found that overexpression of the activated form of ARA6 ($ARA6^{Q93L}$), which is associated with accelerated formation of the callosic haustorial encasement, repressed the full proliferation of *G. orontii*, but overexpression of activated ARA7 ($ARA7^{Q69L}$) did not have this effect. ARA6 could thus be a novel target in developing tools to overcome this plant disease.

Materials and methods

Plant materials

The mutant *Arabidopsis thaliana* plants used in this study (*ara6-1*, *vamp727*, and *eds16*) have been described previously (Ebine et al. 2008; Haas et al. 2007; Wildermuth et al. 2001). Transgenic plants expressing $ARA6^{Q93L}$, $ARA7^{Q69L}$, $ARA6^{Q93L}$ conjugated with green fluorescent protein (GFP, $ARA6^{Q93L}$-GFP), and GFP-$ARA7^{Q69L}$ were generated as described previously (Ebine et al. 2011; Goh et al. 2007).

Pathogen inoculation and disease resistance scores

For the *Golovinomyces orontii* susceptibility assay, 4-week-old *A. thaliana* plants were inoculated with *G. orontii* conidiospores as described previously (Inada and Savory 2011). Counting of conidiophores at 5 days post inoculation (dpi) was also performed as described previously (Inada and Savory 2011).

Quantitative RT-PCR

G. orontii–infected and uninfected leaves were harvested and frozen in liquid N_2 at 7 dpi. Total RNA was extracted using TRIzol according to the manufacturer's protocol. cDNA was synthesized from 1 μg of RNA using a 20 nucleotide OligodT primer and ReverTra Ace reverse transcriptase (TOYOBO, Osaka, Japan), and a 1/10 concentration of cDNA was used for semi-quantitative RT-PCR and qRT-PCR with *PR1*-specific primers (PR1F: 5′-GTA GGT GCT CTT GTT CTT CCC-3′, PR1R: 5′-CAC ATA ATT CCC ACG AGG ATC-3′) and actin (*ACT8*)-specific primers (ACT8F: 5′-TTT ACG CCA GTG GTC GTA C-3′, ACT8R: 5′-TCC GAG TTT GAA GAG GCT AC-3′). qRT-PCR was performed using a Light Cycler 480 SYBR Green I Master and a Light Cycler System (Roche Diagnostics, Basel, Switzerland). Expression levels of *PR1* were normalized with those of *ACT8*.

Observation of callosic encasement

For the observations of the haustorial encasements, leaves were collected from at least two plants (at least two leaves from each plant) and soaked in 99% ethanol at each time point. The cleared leaves were incubated in 0.07 M sodium phosphate buffer (pH 9.0) for 30 min and then stained with 0.05% aniline blue in 0.07 M sodium phosphate buffer, pH 9.0, for 1 h. The aniline blue–stained samples were excited with a UV lamp and observed under a Zeiss Axioplan2 microscope (Zeiss, Oberkochen, Germany).

Confocal microscopy

G. orontii–infected leaves were stained with propidium

iodide (PI) as described previously (Koh et al. 2005) and then observed using a Leica confocal system equipped with 20× N.A. 0.7 and 63× N.A. 1.4 objective lenses (TCS-SP5, Leica Microsystems, Wetzlar, Germany). GFP fluorescence was excited at 488 nm and monitored with a band-pass filter at 500 nm to 550 nm, and the PI was excited at 561 nm and monitored with a band-pass filter from 580 nm to 650 nm. The images were reconstructed and analyzed using ImageJ64 version 1.46f (http://rsbweb.nih.gov/ij/).

Statistical analysis

Results are expressed as the mean±standard error from an appropriate number of experiments as indicated in the figure legends. Student's *t*-test was used to analyze statistical significance.

Results

ARA6 is responsible for full pathogenicity of Golovinomyces orontii

Our previous confocal microscope analyses revealed that both ARA6 and ARA7 accumulate at the EHM formed by *G. orontii*, and that this RAB5 accumulation is positively correlated with the function of the haustorium (Inada et al. 2016a). To examine the role of RAB5s in plant–powdery mildew fungus interactions, we investigated the susceptibility of a series of RAB5-related mutants and transgenic plants to *G. orontii*.

RAB GTPase functions as a molecular switch by cycling between activated GTP-bound and inactivated GDP-bound states, and it mediates the tethering and fusion of the transport vesicles (Inada and Ueda 2014). Guanine nucleotide exchange factor (GEF) catalyzes the activation of RAB by exchanging GDP on RAB for GTP, and VPS9a (At3g19770) is the sole activating factor for all RAB5 members in the vegetative tissues of *A. thaliana* (Goh et al. 2007). VAMP727 (At3g54300) is a soluble *N*-ethylmaleimide-sensitive factor attachment protein receptor (SNARE) protein that is responsible for the fusion of endosomes with the vacuoles and the plasma membrane under the regulation of canonical RAB5 and plant-unique ARA6, respectively (Ebine et al. 2008; Ebine et al. 2011). We examined the susceptibility of *ara6*, *ara6*/*vamp727*, and *vps9a-2* mutants by counting the number of conidiophores per colony at 5 dpi (Figure 1A). Both *ara6* and *ara6*/*vamp727* showed levels of *G. orontii* proliferation comparable to that on the wild type (Figure 1A). A complete knockout mutant of *VPS9a* becomes lethal, so we used the leaky mutant allele *vps9a-2*, in which truncated protein is expressed at a lower expression level (Goh et al. 2007). *vps9a-2* also exhibited no significant changes in susceptibility to *G. orontii* (Figure 1A).

Conversely, in transgenic plants overexpressing the constitutively active form of ARA6 under the CaMV 35S promoter, ARA6^{Q93L}OX (Ebine et al. 2011; Goh et al. 2007), the number of conidiophores produced by *G. orontii* was significantly reduced compared with Col-0 plants (Figure 1A). This increased-resistance phenotype

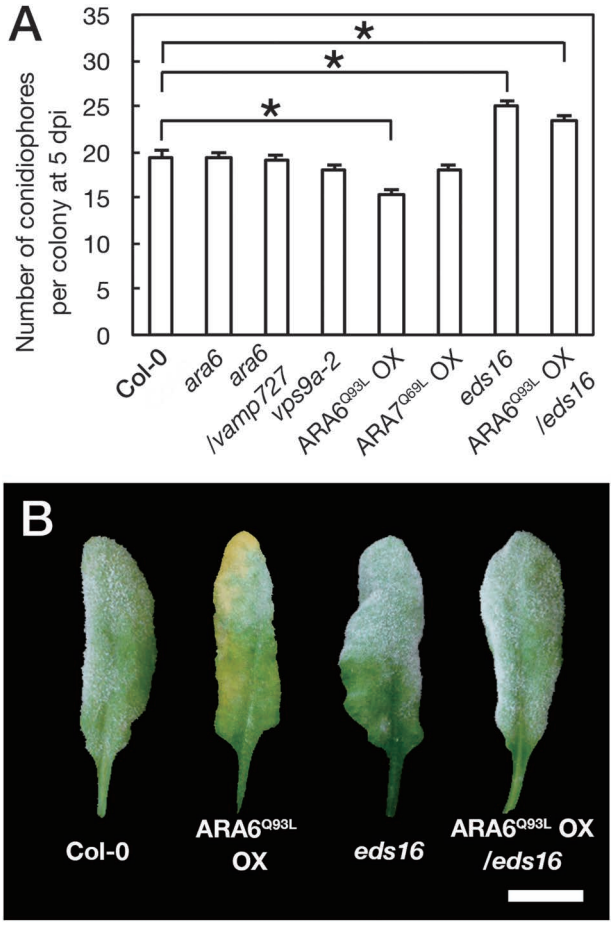

Figure 1. Overexpression of activated ARA6 enhances resistance to *Golovinomyces orontii*. A, Number of conidiophores per colony that formed on Col-0, *ara6-1*, *ara6-1/vamp727*, *vps9a-2*, ARA6^{Q93L} OX, ARA7^{Q69L} OX, *eds16*, and ARA6^{Q93L} OX/*eds16* plants at 5 days post inoculation (dpi). The results are presented as the mean of 100 colonies±standard errors. *$p<0.01$, Student's *t*-test. Experiments were repeated three times, and all replicates yielded similar results. B, Leaves of Col-0, ARA6^{Q93L} OX, *eds16*, and ARA6^{Q93L} OX/*eds16* plants at 2 weeks post inoculation. Scale bar, 1 cm.

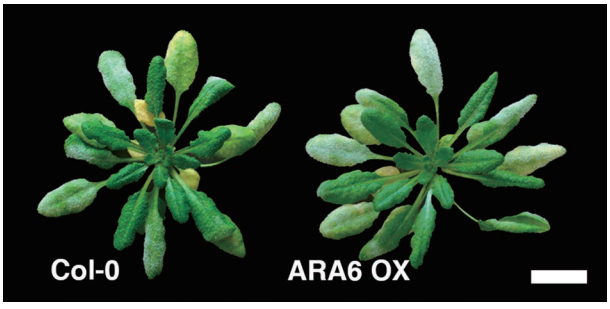

Figure 2. Susceptibility to *G. orontii* was not altered by overexpressing wild-type ARA6 under the regulation of the CaMV 35S promoter (ARA6 OX). Scale bar, 1 cm.

was further examined by visually evaluating the mycelial coverage on leaves at 2 weeks post inoculation (wpi). ARA6^{Q93L} OX exhibited leaf yellowing, a sign of increased plant immunity, with reduced mycelial coverage at 2 wpi (Figure 1B). The plants overexpressing wild-type ARA6 did not exhibit altered susceptibility to *G. orontii* (Figure 2).

By contrast, the equivalent mutant of conventional RAB5, ARA7^{Q69L} OX (Goh et al. 2007), exhibited powdery mildew susceptibility comparable to Col-0 (Figure 1A). This result indicates that the trafficking pathway that is regulated by ARA6, or the activity of ARA6 itself, rather than ARA7 activity, is responsible for the optimal proliferation of *G. orontii*.

Formation of the haustorial encasement is accelerated in plants overexpressing activated ARA6

Upregulation of the salicylic acid (SA)-mediated host defense mechanism confers inhibitory effects on *G. orontii* proliferation (Wildermuth et al. 2001). We therefore examined whether the inhibitory effect of ARA6^{Q93L} OX on *G. orontii* proliferation is mediated by SA. The RT-PCR analysis of the *PR1* gene, which has been shown to exhibit an increased expression level in response to SA (Inada et al. 2016b; Wildermuth et al. 2001), revealed no hyper-activation of the SA-mediated defense response by ARA6^{Q93L} OX in the examined time frame (Figure 3). However, introduction of the mutation in *EDS16* (At1g74710), which encodes an SA biosynthetic enzyme (Wildermuth et al. 2001), completely reversed the effect of ARA6^{Q93L} OX on *G. orontii* proliferation (Figures 1A and 1B), indicating that SA signaling mediates the suppression of *G. orontii* proliferation in ARA6^{Q93L} OX plants.

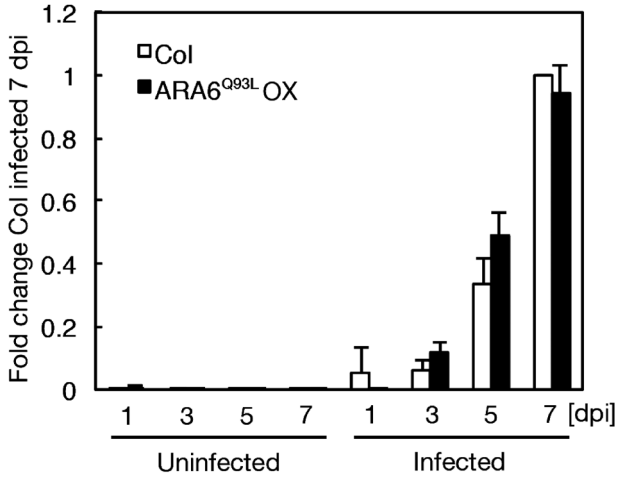

Figure 3. Quantitative RT-PCR analysis of *PR1* in *G. orontii*–infected and uninfected wild-type (Col-0) and ARA6^{Q93L} OX plants. The quantitative PCR analysis of the expression of *PR1* was performed, and normalized with the expression level of *ACT8*, in uninfected and *G. orontii*–infected leaves of wild-type and ARA6^{Q93L} OX plants at 1, 3, 5, and 7 dpi. Experiments were repeated twice, and no significant differences in the expression levels were detected between ARA6^{Q93L} OX and the wild type.

We then examined whether the enhanced immunity in ARA6^{Q93L} OX was targeted to the haustorium. Although the morphologies of the haustoria that formed in the ARA6^{Q93L} OX plants were indistinguishable from those that formed in the Col-0 plants, we observed that the formation of the haustorial encasement was accelerated in ARA6^{Q93L} OX (Figures 4A and 4B). In the primary infected cells, a significantly larger proportion of encased haustoria was observed in ARA6^{Q93L} OX plants at 2 dpi compared with Col-0 plants (Figure 4C), whereas significant differences in encasement formation were not observed at 3 dpi (Figure 4C). The accelerated haustorial encasement formation at 2 dpi in the ARA6^{Q93L} OX plants was suppressed by the *eds16* mutation (Figure 4C).

The constitutively active form of ARA6, but not ARA7, accumulates at the EHM

The above results suggest that the overexpression of ARA6^{Q93L} caused a qualitative alteration of the EHM, which led to an enhanced SA-mediated defense response and accelerated haustorial encasement formation. If this is the case, ARA6^{Q93L} should be targeted to the EHM, as is the case with wild-type ARA6.

ARA6^{Q93L}-GFP was previously reported for its localization on the vacuolar membrane (Ebine et al. 2011; Ueda et al. 2001). The host cytosol surrounding the haustorium is generally very thin, less than 200 nm, and the distance between the vacuolar membrane and the EHM is below the resolution limit of the light microscope. We previously developed a method to distinguish EHM-localized GFP from GFP localized on the vacuolar membrane with confocal microscopy by observing haustoria located near the host cell periphery or close to the host nucleus. Those haustoria were surrounded by the vacuolar membrane only partially, whereas the GFP localized on the EHM thoroughly surround the haustorium (Inada et al. 2016a).

When the haustoria near the cell periphery and those associated with the host nucleus were observed, ARA6^{Q93L}-GFP thoroughly surrounded the haustoria in both cases, a pattern expected for the EHM (Figures 5A and 5C). ARA6^{Q93L}-GFP also showed localization to the vacuolar membrane in accordance with the previous report (Figure 5A). By contrast, GFP-ARA7^{Q69L} exhibited typical patterns of vacuolar membrane localization (Figures 5B and 5D). This result is consistent with the absence of detectable effects of ARA7^{Q69L} overexpression on *G. orontii* proliferation.

Discussion

Previously, we showed that the EHM of haustoria formed

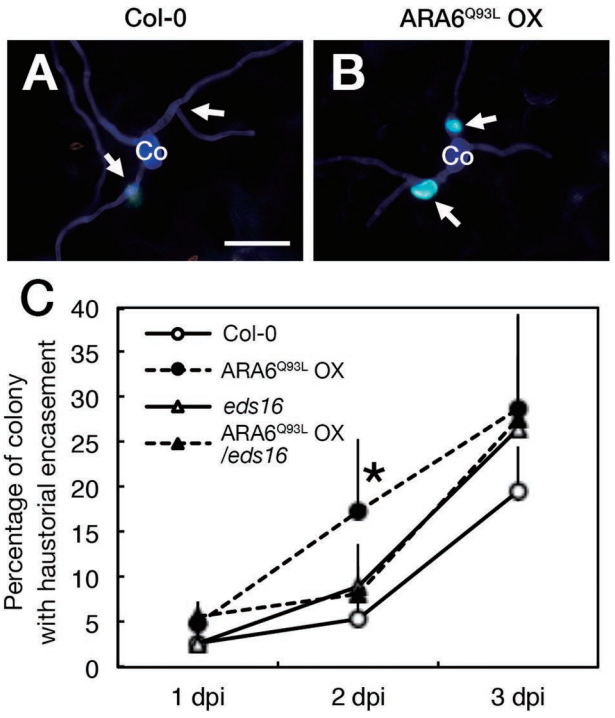

Figure 4. *G. orontii* haustoria in ARA6^{Q93L} OX leaves are encased by haustorial encasements at an earlier infection stage. A, B, Fluorescence micrographs of aniline blue–stained leaves of *G. orontii*–infected Col-0 (A) and ARA6^{Q93L} OX (B) plants at 2 dpi. Arrows indicate haustoria and haustorial encasements. Co, conidium. Scale bar, 50 μm. C, The percentages of colonies with haustorial encasement formation in primary infected cells at 1 to 3 dpi. The results are presented as the mean±standard deviation (mean is the average of three independent experiments; 100 colonies were examined in each experiment). * $p<0.05$, Student's *t*-test.

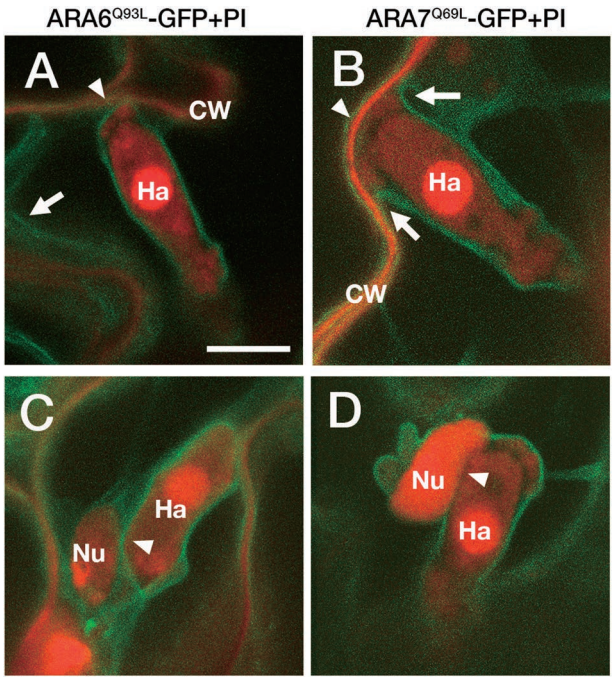

Figure 5. Localization of ARA6^{Q93L}-GFP and GFP-ARA7^{Q69L} around the *G. orontii* haustorium stained with propidium iodide (PI). A, B, Haustoria located near the cell wall. Maximum intensity projection of serial confocal sections of ARA6^{Q93L}-GFP (A), and a single confocal section of GFP-ARA7^{Q69L} (B). Arrowheads indicate the sites at which the haustoria are located close to the host cell wall (CW). Arrows indicate ARA6^{Q93L}-GFP and GFP-ARA7^{Q69L} localized on the tonoplast. C, D, Haustoria associated with host nuclei. Maximum intensity projection of serial confocal sections of ARA6^{Q93L}-GFP (C), and a single confocal image of GFP-ARA7^{Q69L} (D). Arrowheads indicate the boundary between the haustorium (Ha) and the nucleus (Nu), both stained with PI. Scale bar, 10 μm.

by obligate biotrophs, including fungi causing powdery mildew and oomycetes causing downy mildew, acquire host-plant-specific ARA6 and canonical ARA7, but not the related SNARE and GEF, indicating modified endosomal identity of the EHM (Inada et al. 2016a). In this study, we demonstrated that the pathway mediated by plant-specific ARA6, but not by canonical ARA7, plays a major role in plant–powdery mildew fungus interaction.

Tests of susceptibility to *G. orontii* revealed that fungal proliferation was significantly reduced by overexpression of constitutively active ARA6 (ARA6^{Q93L}) but not by overexpression of constitutively active ARA7 (ARA7^{Q69L}). Although overexpression of ARA6^{Q93L} did not cause significant changes in the expression level of *PR1*, the reduced *G. orontii* proliferation phenotype was suppressed by the *eds16* mutation. This result indicates that SA-mediated immunity contributes to the repression of *G. orontii* proliferation in ARA6^{Q93L} OX. Together with the accelerated formation of callosic encasement in ARA6^{Q93L} OX, we speculate that SA-mediated immunity is activated only transiently in limited areas, probably in infected cells, and thus its activation in ARA6^{Q93L} OX could not be detected by qRT-PCR using whole leaves.

The endocytic/vacuolar transport pathways in *A. thaliana*, which transport cargoes to the vacuole, involve both ARA6 and ARA7 as mentioned in the Introduction section. During the trafficking, endosomes mature from RAB5-positive endosomes to RAB7-positive endosomes, which requires the activation of RAB5 catalyzed by the RAB5 GEF (Cui et al. 2014; Ebine et al. 2014; Rink et al. 2005; Singh et al. 2014). The absence of VPS9a, VAMP727 and RAB7 on the EHM, and the presence of ARA6 (Inada et al. 2016a), could reflect a unique endosomal characteristic of the EHM, which is maintained in a maturation-incompetent state. It is possible that in ARA6^{Q93L} OX, the EHM is forced to undergo endosomal maturation, which may interfere with haustorium functions such as suppression of host immunity. Similarly, it was previously reported that the *Rhizobium* symbiosome is maintained in a unique late endosomal stage, acquiring the late endosomal marker RAB7 and excluding vacuolar membrane markers SYP22 and VTI11 until the onset of senescence. The expression of constitutively activated RAB7 caused premature senescence of nodules, thus the authors proposed that

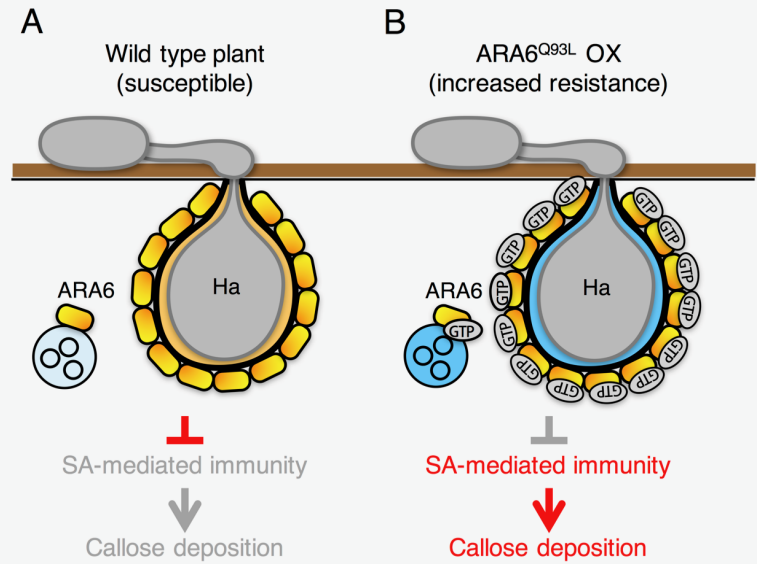

Figure 6. A schematic diagram of the ARA6 function in plant-powdery mildew fungus interaction. A, A wild type plant infected by *G. orontii*. The functional haustorium (Ha), which is surrounded by the ARA6-localized extrahaustorial membrane, suppresses salicylic acid (SA)-mediated immunity and callose deposition. B, An ARA6^{Q93L} OX plant infected by *G. orontii*. In this plant, the suppressive function of the haustorium against the plant immunity is interfered by ARA6^{Q93L} on the extrahaustorial membrane. This interference might result in accelerated callose deposition around the haustorium.

symbiosomes are locked in the late-endosomal state to delay the acquisition of lytic vacuolar identity and thus to ensure the survival of symbiosomes in the host cells (Limpens et al. 2009).

A schematic summary of our study is shown in Figure 6. In wild type plants, *G. orontii* can form functional haustoria, which are surrounded by the ARA6-bearing EHM. The functional haustoria suppress SA-mediated plant immunity, leading to suppression of callose deposition around the haustoria at an early infection stage. Conversely, in plants overexpressing ARA6^{Q93L}, which mimics the GTP-bound active form of ARA6, the EHM with ARA6^{Q93L} interferes a function of the haustoria, which results in temporal and localized enhancement in plant immunity in *G. orontii*-infected cells. As a result of the activated immunity, the callosic encasement is formed at the early infection stage. The formation of the callosic encasement could further enhance inhibition of the haustorial function, resulting in compromised proliferation of *G. orontii*.

Because the *ara6* mutant exhibited no detectable changes in *G. orontii* proliferation compared with wild-type plants, other RAB GTPases, such as conventional RAB5 or other endosomal RABs, could also be involved in plant–powdery mildew fungus interactions. Indeed, for mammal-infecting bacteria that are known to manipulate host RAB GTPases for infection, it has been shown that many different RAB GTPases are recruited to the host-derived membrane that surrounds the bacteria, and for many of these RAB GTPases there is no effect on bacterial proliferation when their expressions are reduced (Dorer et al. 2006; Urwyler et al. 2009).

We previously showed that accumulation of ARA6 on the EHM is a common feature in plant and haustorium-forming pathogen interactions (Inada et al. 2016a). In addition to exhibiting resistance to plant pathogens, plants that overexpress ARA6^{Q93L} also exhibit increased resistance to salinity stress (Ebine et al. 2011). Manipulation of ARA6 activity could be an efficient methodology for producing plants resistant to multiple stresses.

Acknowledgements

We thank Ms. S. Nakagawa (NAIST) and Mr. T. Inoue (University of Tokyo) for technical assistance. This work was supported by Grants-in-Aid for Scientific Research from the Ministry of Education, Culture, Sports, Science, and Technology of Japan (16K07415 to NI and 24114003 and 15H04382 to TU), Grants-in-Aid for Scientific Research from NAIST (NI), and JST, PRESTO (JPMJPR11B2 to TU).

References

Acevedo-Garcia J, Kusch S, Panstruga R (2014) Magical mystery tour: MLO proteins in plant immunity and beyond. *New Phytol* 204: 273–281

Bottanelli F, Foresti O, Hanton S, Denecke J (2011) Vacuolar transport in tobacco leaf epidermis cells involves a single route for soluble cargo and multiple routes for membrane cargo. *Plant Cell* 23: 3007–3025

Cui Y, Zhao Q, Gao C, Ding Y, Zeng Y, Ueda T, Nakano A, Jiang L (2014) Activation of the Rab7 GTPase by the MON1-CCZ1 complex is essential for PVC-to-vacuole trafficking and plant growth in Arabidopsis. *Plant Cell* 26: 2080–2097

Dorer MS, Kirton D, Bader JS, Isberg RR (2006) RNA interference analysis of *Legionella* in Drosophila cells: exploitation of early

secretory apparatus dynamics. *PLoS Pathog* 2: e34
Ebine K, Fujimoto M, Okatani Y, Nishiyama T, Goh T, Ito E, Dainobu T, Nishitani A, Uemura T, Sato MH, et al. (2011) A membrane trafficking pathway regulated by the plant-specific RAB GTPase ARA6. *Nat Cell Biol* 13: 853–859
Ebine K, Inoue T, Ito J, Ito E, Uemura T, Goh T, Abe H, Sato K, Nakano A, Ueda T (2014) Plant vacuolar trafficking occurs through distinctly regulated pathways. *Curr Biol* 24: 1375–1382
Ebine K, Okatani Y, Uemura T, Goh T, Shoda K, Niihama M, Morita MT, Spitzer C, Otegui MS, Nakano A, et al. (2008) A SNARE complex unique to seed plants is required for protein storage vacuole biogenesis and seed development of *Arabidopsis thaliana*. *Plant Cell* 20: 3006–3021
Ebine K, Ueda T (2009) Unique mechanism of plant endocytic/vacuolar transport pathways. *J Plant Res* 122: 21–30
Goh T, Uchida W, Arakawa S, Ito E, Dainobu T, Ebine K, Takeuchi M, Sato K, Ueda T, Nakano A (2007) VPS9a, the common activator for two distinct types of Rab5 GTPases, is essential for the development of *Arabidopsis thaliana*. *Plant Cell* 19: 3504–3515
Haas TJ, Sliwinski MK, Martinez DE, Preuss M, Ebine K, Ueda T, Nielsen E, Odorizzi G, Otegui MS (2007) The Arabidopsis AAA ATPase SKD1 is involved in multivesicular endosome function and interacts with its positive regulator LYST-INTERACTING PROTEIN5. *Plant Cell* 19: 1295–1312
Inada N, Betsuyaku S, Shimada TL, Ebine K, Ito E, Kutsuna N, Hasezawa S, Takano Y, Fukuda H, Nakano A, et al. (2016a) Modulation of plant RAB GTPase-mediated membrane trafficking pathway at the interface between plants and obligate biotrophic pathogens. *Plant Cell Physiol* 57: 1854–1864
Inada N, Higaki T, Hasezawa S (2016b) Nuclear function of subclass I actin depolymerizing factor contributes to susceptibility in Arabidopsis to an adapted powdery mildew fungus. *Plant Physiol* 170: 1420–1434
Inada N, Savory EA (2011) Inhibition of prepenetration processes of the powdery mildew *Golovinomyces orontii* on host inflorescence stems is reduced in the *Arabidopsis* cuticular mutant *cer3* but not in *cer1*. *J Gen Plant Pathol* 77: 237–281
Inada N, Ueda T (2014) Membrane trafficking pathways and their roles in plant-microbe interactions. *Plant Cell Physiol* 55: 672–686
Koh S, Andre A, Edwards H, Ehrhardt D, Somerville S (2005) *Arabidopsis thaliana* subcellular responses to compatible *Erysiphe cichoracearum* infections. *Plant J* 44: 516–529
Kotzer AM, Brandizzi F, Neumann U, Paris N, Moore I, Hawes C (2004) AtRabF2b (Ara7) acts on the vacuolar trafficking pathway in tobacco leaf epidermal cells. *J Cell Sci* 117: 6377–6389
Limpens E, Ivanov S, van Esse W, Voets G, Fedorova E, Bisseling T (2009) Medicago N2-fixing symbiosomes acquire the endocytic identity marker Rab7 but delay the acquisition of vacuolar identity. *Plant Cell* 21: 2811–2828
Meyer D, Pajonk S, Micali C, O'Connell R, Schulze-Lefert P (2009) Extracellular transport and integration of plant secretory proteins into pathogen-induced cell wall compartments. *Plant J* 57: 986–999
Rink J, Ghigo E, Kalaidzidis Y, Zerial M (2005) Rab conversion as a mechanism of progression from early to late endosomes. *Cell* 122: 735–749
Singh MK, Kruger F, Beckmann H, Brumm S, Vermeer JE, Munnik T, Mayer U, Stierhof YD, Grefen C, Schumacher K, et al. (2014) Protein delivery to vacuole requires SAND protein-dependent Rab GTPase conversion for MVB-vacuole fusion. *Curr Biol* 24: 1383–1389
Sohn EJ, Kim ES, Zhao M, Kim SJ, Kim H, Kim YW, Lee YJ, Hillmer S, Sohn U, Jiang L, et al. (2003) Rha1, an Arabidopsis Rab5 homolog, plays a critical role in the vacuolar trafficking of soluble cargo proteins. *Plant Cell* 15: 1057–1070
Takamatsu S (2004) Phylogeny and evolution of the powdery mildew fungi (Erysiphales, Ascomycota) inferred from nuclear ribosomal DNA sequences. *Mycosci* 45: 147–157
Ueda T, Uemura T, Sato MH, Nakano A (2004) Functional differentiation of endosomes in Arabidopsis cells. *Plant J* 40: 783–789
Ueda T, Yamaguchi M, Uchimiya H, Nakano A (2001) Ara6, a plant-unique novel type Rab GTPase, functions in the endocytic pathway of *Arabidopsis thaliana*. *EMBO J* 20: 4730–4741
Urwyler S, Nyfeler Y, Ragaz C, Lee H, Mueller LN, Aebersold R, Hilbi H (2009) Proteome analysis of *Legionella* vacuoles purified by magnetic immunoseparation reveals secretory and endosomal GTPases. *Traffic* 10: 76–87
Wildermuth MC, Dewdney J, Wu G, Ausubel FM (2001) Isochorismate synthase is required to synthesize salicylic acid for plant defence. *Nature* 414: 562–565
Xiao S, Ellwood S, Calis O, Patrick E, Li T, Coleman M, Turner JG (2001) Broad-spectrum mildew resistance in *Arabidopsis thaliana* mediated by RPW8. *Science* 291: 118–120
Yi M, Valent B (2013) Communication between filamentous pathogens and plants at the biotrophic interface. *Annu Rev Phytopathol* 51: 587–611